Title
Enhancing the effects of chemotherapy by combined macrophage-mediated photothermal therapy (PTT) and photochemical internalization (PCI)

Journal
Lasers in Medical Science, 33(8)

ISSN
0268-8921

Authors
Nair, Rohit Kumar
Christie, Catherine
Ju, David
et al.

Publication Date
2018-11-01

DOI
10.1007/s10103-018-2534-5

Peer reviewed

HHS Public Access

Author manuscript

Lasers Med Sci. Author manuscript; available in PMC 2019 November 01.

Published in final edited form as:

Lasers Med Sci. 2018 November ; 33(8): 1747–1755. doi:10.1007/s10103-018-2534-5.

Enhancing the effects of chemotherapy by combined macrophage-mediated photothermal therapy (PTT) and photochemical internalization (PCI)

Rohit Kumar Nair[1], **Catherine Christie**[1], **David Ju**[1], **Diane Shin**[1], **Aftin Pomeroy**[1], **Kristian Berg**[2], **Qian Peng**[3], and **Henry Hirschberg**[1]

[1]Beckman Laser Institute and Medical Clinic, University of California, 1002 Health Sciences Rd, Irvine, CA, 92617, USA.

[2]Department of Radiation Biology, University of Oslo, Montebello, 0310, Oslo, Norway.

[3]Pathology Clinic, Rikshospitalet-Radiumhospitalet HF Medical Center, University of Oslo, Montebello, 0310, Oslo, Norway.

Abstract

Light-based treatment modalities such as photothermal therapy (PTT) or photochemical internalization (PCI) have been well documented both experimentally and clinically to enhance the efficacy of chemotherapy. The main purpose of this study was to examine the cytotoxic effects of silica–gold nanoshell (AuNS)-loaded macrophage-mediated (Ma^{NS}) PTT and bleomycin BLMPCI on monolayers of squamous cell carcinoma cells. The two modalities were applied separately and in simultaneous combination. Two different wavelengths of lig7ht were employed simultaneously, one to activate a highly efficient PCI photosensitizer,$AlPcS_{2a}$ (670 nm) and the other for the Ma^{NS}-mediated PTT (810 nm), to evaluate the combined effects of these modalities. The results clearly demonstrated that macrophages could ingest sufficient numbers of silica–gold nanoshells for efficient near infrared (NIR) activated PTT. A significant synergistic effect of simultaneously applied combined PTT and PCI, compared to each modality applied separately, was achieved. Light-driven therapies have the advantage of site specificity, non-invasive and nontoxic application, require inexpensive equipment and can be given as repetitive treatment protocols.

Keywords

Squamous cell carcinoma; Photochemical internalization; Photothermal therapy; Gold-silica nanoshells; Ratmacrophages

Introduction

Systemic chemotherapy is one of the main pillars of modern oncology and its use has resulted in a reduced recurrence rate and improved survival for a wide variety of cancer patients. Most chemotherapeutic agents demonstrate a high efficacy with a variety of tumors but nonspecific delivery methods lead to significant normal tissue toxicities and severe undesirable side effects. These in turn limit systemic drug dosages to levels below those required for curative treatment. Increasing the therapeutic index of chemotherapy by the

development of targeted and localized drug enhancing or activation methods would do much to alleviate many devastating side effects. Externally applied physical targeting methods have the potential of maintaining an increased drug efficacy at the tumor site, allowing significantly lowered systemic drug dosages to be used. The light-based treatment modality, photochemical internalization (PCI), has been well documented both experimentally and clinically to enhance the efficacy of chemotherapy in a site and temporally specific manner [1–5]. Many anticancer agents are limited in their ability to penetrate cell membrane structures and are transported into cells by endocytosis, resulting in their accumulation in intracellular endocytic vesicles (endosomes and lysosomes).

PCI is based on the use of specially designed photosensitizers, with two sulfonate groups on adjacent phenyl rings, such as $TPPS_{2a}$, $AlPcS_{2a}$, and $TPCS_{2a}$ that localize preferentially in the membranes of endocytic and lysosomal intracellular vesicles. Upon exposure to light of appropriate wave lengths, the photosensitizers induce the formation of reactive oxygen species (ROS) including singlet molecular oxygen, leading to the release of the contents of these vesicles into the cell cytosol. The released drugs can now exert their full biological activity instead of being degraded by lysosomal hydrolases. In addition to the toxic effect of the released drug, lysosomal enzymes are also released triggering cell apoptosis. In particular, PCI of Bleomycin (BLM) has proven highly effective in a host of in vitro and in vivo models and was used in a clinical study on head and neck tumors [6–10].

A second light-based targeting method, photothermal therapy (PTT) has also been shown to enhance the efficacy of free drug [11–14]. PTT employs exogenous near infrared (NIR) activated heating agents such as dyes or in particular, silica–gold nanoshells (AuNS), to induce locally targeted moderate hyperthermia via the conversion of NIR radiation to heat [15–17]. AuNS are composed of a dielectric core (silica) coated with an ultrathin gold layer and can absorb or scatter light at NIR wavelengths, a light region in which optical penetration through tissue is optimal. AuNS convert absorbed NIR to heat with an efficacy and stability that far exceeds that of conventional dyes [18–20]. These above-mentioned light-driven therapies have the advantage of site specificity, non-invasive and non-toxic application, require inexpensive equipment and can be given as repetitive treatment protocols.

One important criterion for nanoparticle-based PTT is the targeted delivery of the AuNS. Previous studies of the effects of PTT-induced moderate hyperthermia (MHT) on drug efficacy have used heat converting nanoparticles, directly incorporated within the tumor cells themselves. This approach however is difficult to facilitate in vivo due to the inefficient transport of photothermal nanoparticles into tumors [21, 22].

An alternative to direct injection of nanoparticles is the use of certain types of cells that are known to track to tumors, as transport delivery vectors [23, 24]. Cell-based vectorization is one method that can target and maintain an elevated concentration of nanoparticles at the tumor site and prevent their spread into normal tissue. Employing macrophages, in conjunction with nanoparticle delivery for PTT has interesting potential for cancer treatment since they are attracted to tumors and in particular into hypoxic and necrotic regions [25–28]. We have previously employed macrophages as delivery vectors for AuNS (designated

Ma^{NS}) for PTT [29–32]. Both PCI and PTT have been demonstrated to enhance the efficacy of BLM, so the possibility of a synergistic effect of combining these treatment forms prompted the present study. Since head and neck tumors are often superficial, light-activated therapies like PCI and PTT can be well suited for treatment of these types of cancer. In the experiments reported here, we have therefore examined the cytotoxic effects of PTT and BLM-PCI on monolayers of squamous cell carcinoma cells. The two modalities were applied separately and in simultaneous combination. Two different wavelengths of light were employed simultaneously, one to activate a highly efficient PCI photosensitizer $AlPcS_{2a}$ (670 nm) and the other for the Ma^{NS}-mediated PTT (810 nm), to evaluate the combined effects of these modalities.

Materials and methods

Cell lines

The human squamous cell carcinoma cell line FaDu (ATCC#HTB-43) and rat alveolar Ma NR8383 (ATCC#CRL-2192) were both obtained from the American Type Culture Collection (Manassas, VA). The cells were cultured in Dulbecco's Modified Eagle Media (DMEM, Gibco, Carlsbad, CA) with high glucose and supplemented with 2 mM L-glutamine, gentamycin (100 mg/ml), and 2% heat-inactivated fetal bovine serum (Gibco) at 37 °C in a 7.5% CO_2 incubator.

Nanoshells

The gold nanoshells (AuNS) used in this study consisted of a 120-nm silica core with a 12–15 nm gold shell (Nanospectra Biosciences, Inc., Houston, Texas). The resultant optical absorption peak was between $\lambda = 790$ and $\lambda = 820$ nm for PEGylated particles. The solutions were found to have an optical density (O.D.) of 1.22 at $\lambda = 795$ nm for PEGylated nanoshells (100× dilution).

Ma-Au NS incubation

NR8383 rat alveolar Ma were seeded in 35-mm cell culture dishes at 1×10^6 Ma in 2 ml of culture medium. The dishes were incubated overnight to allow the cells to settle and adhere to the plastic. Culture medium was exchanged for 100 μl of PEGylated (2.8×10^{11} particles/ml) nanoshells colloid in 1.9ml of culture medium. The Ma were incubated for 24 h at 37 °C, rinsed three times with Hanks' Balanced Salt Solution with calcium chloride and magnesium chloride (HBSS, Gibco, Carlsbad, CA) to wash away the excess of noningested nanoshells. Au Nanoshell laden Ma (designated Ma^{NS}) were then detached with trypsin and a rubber spatula, washed, and counted. The concentration of nanoshells in macrophages was studied using a UV-Vis-NIR spectrophotometer (Varian UV-Vis-NIR spectrophotometer Cary 6000i, Varian, USA).

Absorbance was measured at a spectrum involving $\lambda = 600–1100$ nm wavelengths, which covers the broad absorption peak of nanoshells ($\lambda = 819$ nm).

PTT or PCI only treatment

All light treatment was performed at a culture temperature of 37 °C. For PTT only treatment, eight wells in a vertical column in 96-well ultra-low adhesion round-bottomed plates (Corning In., NY) were seeded with either Ma, Ma^{NS} or FaDu+Ma^{NS} (ratio 2:1) cells at a total density of 6×10^3 cells per well. The plates were centrifuged at 1000 G for 10 min to force the cells into a small disk at the bottom of the well and incubated for 24 h prior to experimentation. Cells were plated into every other column (eight wells) in order to minimize the contribution of light scatter between cultures. For PTT, individual wells were irradiated with $\lambda = 810$ nm laser light (Coherent Inc., Santa Clara, CA) at irradiances ranging from 0 to 28W/cm^2 with a beam diameter of approximately 3 mm. Laser exposure interval of 6 min was used.

For PCI only treatment, FaDu+Ma^{NS} cells at various ratios were incubated with 0.5 μg/ml of the photosensitizer $AlPcS_{2a}$ (Frontier Scientific, Inc., Logan, UT) and DMEM for 18 h and washed four times. BLM at increasing concentrations was added in fresh medium. Four hours after BLM was added, light treatment, $\lambda = 670$ nm, from a diode laser (Intense, North Brunswick, NJ) at an irradiance of 2.0 mW/cm^2 was administered for 6 or 8 min, corresponding to radiant exposures of 0.72 or 0.96 J/cm^2 respectively. Control cultures received light treatment but no BLM (PDT control) or BLM but no illumination (drug only control). Following PCI, the plates were returned to the incubator. Following either PTT or PCI laser irradiance, incubation was continued for 48 h, at which point the culture medium was replaced with fresh clear buffer containing MTS (3-(4,5-dimethylthiazol-2-yl)-5-(3-carboxymethoxyphenyl)-2-(4-sulfophenyl)-2H-tetrazolium MTS, Promega, Madison, WI) reagents and incubated for an additional 2 h. The optical density was measured using an ELx800uv Universal Microplate Reader (Bio-Tek Instruments, Inc., Winooski, VT). Since the NR8383 Ma are normal cells and have a very low mitotic rate compared to the FaDu cells, growth in the post treatment interval (48 h) was considered predominantly due to the FaDu tumor cells.

Combined PCI-PTT treatment

Figure 1 shows the setup for the two wavelength light treatment. FaDu and Ma^{NS} were combined at a ratio of FaDu:Ma^{NS} of 2:1. One hundred microliter of medium containing 6×10^3 cells were aliquoted into the wells of ultra-low adherence round-bottomed plates and the plates were centrifuged at 1000 G for 10 min as previously described. $AlPcS_{2a}$ (0.5 μl/ml) was added to each well, and the plates incubated for 18 h. The cells were washed four times to remove excess photosensitizer, BLM at concentrations of 0, 0.3, and 0.6 mg/ml and the plates incubated for an additional 4 h. Individual wells were irradiated with either $\lambda = 810$ nm, $\lambda = 670$ nm or a combination of the two wavelengths. $\lambda = 670$ nm irradiation, both alone and combined, was performed through a 1-cm opaque mask that allowed only one well at a time to be treated. For combined treatment, the wells were irradiated simultaneously, $\lambda = 670$ nm from above, $\lambda = 810$ nm from below. Following laser irradiance, incubation was continued for 48 h and cell survival was assayed by MTS assay as previously described.

Statistical analysis

Microsoft Excel was employed for the calculation of the arithmetic mean, standard deviation, and standard error. Experimental data were analyzed using one-way analysis of variance (ANOVA) at the significance level of $p < 0.05$ and presented as mean with standard error unless otherwise noted. Synergistic effects were calculated for combined PTT-PCI treatments compared to PTT or PDT alone. The equation shown below was used to determine if the combined effect was synergistic, antagonistic, or additive, where Bα^ is the ratio of the cumulative effect of two therapies administered independently to the net effect of combining the two therapies at a given dose.

$$\alpha = \frac{SF^{PTT} \times SF^{PCI}}{SF^{PTT+PCI}}$$

In this scheme, SF represents the survival fraction for a specific treatment. If $\alpha > 1$, the result is synergistic (supra-additive). If $\alpha < 1$, the result is antagonistic, and if $\alpha = 1$, the result is simply additive.

Results and discussion

Macrophage endocytosis of PEGylated nanoshells

Nanoparticles are often coated with polyethylene glycol (PEGylation) to prevent their rapid elimination from the circulation by the reticuloendothelial system and to inhibit their propensity to aggregate. The ability of the rat alveolar macrophages used in this study to take up PEGylated AuNS was determined by UV-Vis-NIR spectrophotometry. The percentage uptake of PEGylated nanoshells in the macrophages was approximately 10%. 1×10^6 Ma incorporated 30×10^8 PEGylated nanoshells. As shown in Fig. 2b, despite thePEGylation of AuNS, they were rapidly and effectively taken up by macrophages. The internalized AuNS in Ma were visualized as dark opaque regions in the phase contrast microscopy images (Fig. 2b). These dark areas are absent in the control “empty” Ma (Fig. 2a). These results are in agreement with the findings of Yang et al. where rat peritoneal macrophages were used with similar AuNS, to those used here [33].

Effects of PTT on FaDu-Ma^{NS}

Since it is theMa^{NS} that convert the NIR laser energy into heat delivering hyperthermia to cancer cells, it was important to determine the effects of PTT on hybrid FaDu-Ma^{NS} directly. FaDu and Ma^{NS} were combined at FaDu:Ma^{NS} ratios of 1:1 or 2:1, the FaDu cell numbers were 4×10^3. The cells were aliquoted and spun down in the wells of non-adherent round-bottomed 96-well plates and were exposed to NIR laser powers of 0, 7, 14 and 28 W/cm^2 delivered with a beam size of 3 mm. The small beam size was necessary in order to achieve the high radiant exposures required in a reasonable time period and with the available laser power. The effects of NIR laser irradiation on FaDu cells in combination with empty Ma or Ma^{NS} are shown in Fig. 3. No significant cytotoxicity was observed for empty Ma in the absence or presence of $AlPcS_{2a}$ even at irradiances of 28 W/cm^2 for 6 min. In contrast, a significant decline in cell viability with increasing irradiance was demonstrated for the

FaDu:MaNS monolayers. At a FaDu:MaNS ratio of 1:1 and 14 W/cm2 irradiance, about 50% of the cells survived, compared to almost a 90% survival with a 2:1 ratio of FaDu: Ma^{NS}. At an irradiance of 28W/cm^2, cell viability was reduced to 22 and 18% of control values at cell ratios of 2:1 and 1:1 respectively. This difference was considered non-significant ($p > 0.05$). Since hyperthermia over 46 °C is toxic to cells in culture it was assumed this temperature was reached for both cell ratios, although direct measurements were not under taken.

Effects of PTT and MHT on BLM toxicity

The direct effects on BLM toxicity of PTT or MHT are shown in Fig. 4a, b. To evaluate the effects of MHT, BLM 0.6 μg/ml was added to the wells containing hybrid monolayers as described above and incubated for 45 min at either 37 or 44 °C. The results are shown in Fig. 4a. PTT was performed with 14 W/cm^2 for 6 min. Although a small increase in the toxicity of the drug was noted, it was not significant ($p > 0.05$) for all of the BLM concentrations tested.

Several recent publications have examined the effects of PTT-induced MHT on the efficacy of a variety of chemotherapeutic drugs, including BLM, both in vivo and in vitro [12, 34–37]. MHT typically occurs in a temperature range of 40 to 44 °C, over intervals ranging from 30 to 60 min and although generally non-toxic to cells, it has been shown to increase the efficacy of a number of cytotoxic drugs. The increase in the toxicity of BLM as seen in Fig. 4a, although not pronounced, was probably due to changes in the cell membrane caused by PTT or external MHT. BLM being water soluble and a large molecule is taken up by endocytosis and is therefore influenced by both cell and endocytic vesicles (endosomes and lysosomes) membrane permeability.

As opposed to BLM, chemotherapeutic agents such as cisplatin or doxorubicin (DOX) are transported into the cell directly through the cell membrane, so membrane permeability directly determines intracellular drug concentration. The significant increase of PTT and external MHT on the efficacy of these drugs, reported in previous publications, lends support to this explanation [11, 13, 35].

PCI of FaDu-Ma^{NS}

In order to determine the cytotoxic effects of combined PTT and BLM-PCI on FaDu cells, it was necessary to establish a suboptimal light and BLM dose to be used in subsequent experiments. 4×10^3 FaDu cells combined with 2×10^3 Ma^{NS} cells were irradiated with λ = 670 nm at increasing radiant exposures 0, 0.48, 0.72, and 0.96 J/cm^2 at irradiances of 2mW/cm^2 (Fig. 4b) corresponding to irradiation times of 4, 6, and 8 min with BLM concentrations of 0, 0.3, 0.6, and 1.2 μg/ml. Radiant exposures of 0.72 and 0.96 in the absence of BLM (PDT control) gave 95 and 63% cell survival respectively. In contrast, at a BLM concentration of 0.6 μg/ml, a moderate (70%) and pronounced (15%) PCI toxic effect was shown at 0.72 and 0.96 J/cm2 respectively (Fig. 4b).

Combined PTT-PCI on FaDu-Ma^{NS} cells

Figure 5a shows the effect PTT on BLM-PCI with increasing light exposure. λ = 670 nm laser irradiance of 0–0.96 J/cm^2 with and without NIR laser irradiance of 14 W/cm^2 and a simultaneous irradiation duration of 6 min for both laser beams. BLM concentration of 0.6 μg/ml and a FaDu:Ma^{NS} ratio of 2:1 were used. As can be seen from the figure, cell viability was 87, 76, and 21% of control values for the three λ =670 nm light radiance levels respectively. The addition of NIR, PTT significantly decreased cell viability to 47, 11, and 10% of control values.

One of the main limitations of both PDT and PCI is the rapid attenuation of light in tissue at the wavelengths used to excite available photosensitizers. In contrast, most biological tissues lack NIR-absorbing chromophores, thus permitting transmission of NIR light at λ =810 nm, to a much greater depth than that obtained with for example λ = 670 nm. The synergistic effect of combined PTT and PCI, as seen in Fig. 5a, would therefore result in an equal PCI drug efficacy to be achieved at significantly reduced light radiation levels. This in turn would produce an effective PCI treatment at a greater depth in tumor tissue.

Figure 5b shows the effect of PTT on BLM-PCI with increasing NIR light exposure. λ = 810 nm laser irradiance of 0–28 W/cm^2 with and without 670-nm laser radiance of 0.72 J/cm^2, and for combined treatment, a simultaneous irradiation duration of 6 min for both laser beams. BLM concentration of 0.6 μg/ml and a FaDu:Ma^{NS} ratio of 2:1 was used. At lower PTT irradiances (7 W/cm^2) no significant increase in the cytotoxic effects of PCI were observed ($p > 0.1$). Optimal results were obtained at a NIR irradiation of 14 W/cm^2 with a decrease in cell viability falling from 67 to 11% of controls ($p < 0.05$) for PTT alone and combined treatment respectively. At higher irradiation (28 W/cm^2), the direct PTT hyperthermic effect and the increase in BLM toxicity by PTT resulted in a cell viability of 32% of control values. The addition of BLMPCI, although significant ($p < 0.05$), was far less dramatic.

As seen in Fig. 3, the direct $AlPcS_{2a}$ PDT effect at λ = 810 nm NIR irradiation (FaDu + empty Ma) was negligible. The effects of PTT on BLM-PCI are therefore probably caused by the PTT-inducedMHT. Experiments were therefore performed to compare the effects of Ma^{NS} mediated PTT with externally applied MHT on the efficacy of BLM-PCI. External MHT was applied at 44 °C for 45 min. PTT + BLM-PCI treatment was done with 14 W/cm^2 NIR irradiation, 0.72 J/cm^2 and 0.6 μg/ml BLM. The results are shown in Fig. 5c. A significant reduction in cell viability compared to controls (53%) was achieved by combined PTT and PDT (no BLM). This observation agrees well with previous published results in particular with those of Trinidad et al. using a similar PTT protocol and FaDu cells [36–38]. Cell viability was additionally significantly reduced by the combination of externally applied MHT (44 °C) and BLM–PCI as seen in Fig. 5c.

This finding agrees well with the work of Christie and coworkers, who could demonstrate an enhanced MHTPCI effect on the growth of glioma spheroids, using two different anticancer agents [39]. As is also seen in Fig. 5c, the combination of Ma^{NS} PTT gave the greatest boost to BLM efficacy. Although the inhibitory effects of PTT + BLM-PCI were slightly more pronounced than that seen with MHT + BLMPCI, the difference was not significant (p >

0.1). This difference might be due to the rate of heat application, rapid heating being more effective than slow heat application, as previously postulated by Tang et al. on the basis of their results demonstrating a difference between PTT and MHT [11].

Quantitative evaluation of simultaneous PTT + BLM-PCI and MHT + BLM-PCI, determined from the degree of interaction (α), was calculated from the data shown in Figs. 4 and 5 and are shown in Table 1. The α values for the effects of combined treatment cytotoxicity for a PTT irradiance of 14 W/cm^2 and radiant exposures of 0.72 J/cm^2, ranged from 1.6 ± 0.14 to 6.3 ± 0.58 for BLM concentrations of 0, 0.3 and 0.6 μg/ml respectively, clearly indicating a synergistic effect.

The toxic PTT effect at a laser power of 28 W/cm2 was so pronounced (Fig. 3) that synergy is masked, as reflected by the low α values in the table.

The mechanism of synergism between PTT-induced MHT and PCI is likely to have three main components. PTT induced MHT increases intracellular BLM concentration by increasing cellular uptake via endocytosis as shown in Fig. 4a.

BLM is incorporated into DNA-causing double strand breaks which induces cell death unless the damage is repaired. Since hyperthermia inhibits DNA repair, it is postulated that the addition of PTT enhances the cytotoxicity of the chemotherapeutic agents via MHT inhibition of DNA repair. Probably the most important effect is that PTT has been demonstrated to increase the cytotoxic effect of PDT in a similar experimental setup [38]. Since PCI is based on the ability of PDT to rupture intracellular photosensitizer containing vesicle membranes, it is reasonable to assume that PTT + PDT will enhance the escape of entrapped BLM. Additionally, PTT alone has been demonstrated to enhance endosomal escape of the drug doxorubicin encapsulated in reduced graphene oxide nano agents [40].

In the experiments reported here, BLM was delivered as free drug dissolved in the culture medium and the macrophages were used only as delivery vehicles for the AuNS. Efficient drug delivery by macrophages has also recently been demonstrated both with and without PCI [41–43]. Macrophages loaded with a combination of drug and AuNS for combined PTT-PCI are now under investigation, both in vitro and in animal models.

Conclusion

The results of the experiments presented here clearly demonstrated that macrophages could ingest sufficient numbers of PEGylated silica–gold nanoshells for efficient NIR activated PTT. A significant synergistic increased efficacy of BLM was achieved by simultaneously applied combined PTT and BLMPCI, compared to each modality applied separately. The addition of NIR-mediated PTT to PCI protocols allows for drug activation at a greater depth in tumor tissue.

Acknowledgments

The authors are grateful for the support from the Norwegian Radium Hospital Research Foundation. Portions of this work were made possible through access to the LAMMP Program NIBIB P41EB015890.

References

1. Berg K, Selbo PK, Prasmickaite L, Tjelle TE, Sandvig K, Moan J, Gaudernack G, Fodstad O, Kjølsrud S, Anholt H, Rodal GH, Rodal SK, Høgset A (1999) Photochemical internalization: a novel technology for delivery of macromolecules into cytosol. Cancer Res 59(6):1180–1183 [PubMed: 10096543]
2. Berg K, Folini M, Prasmickaite L, Selbo PK, Bonsted A, Engesaeter BØ, Zaffaroni N, Weyergang A, Dietze A, Maelandsmo GM, Wagner E, Norum OJ, Høgset A (2007) Photochemical internalization: a new tool for drug delivery. Curr Pharm Biotechnol 8(6):362–372 [PubMed: 18289045]
3. Norum OJ, Giercksky KE, Berg K (2009) Photochemical internalization as an adjunct to marginal surgery in a human sarcoma model. Photochem Photobiol Sci 8(6):758–762 [PubMed: 19492102]
4. Selbo PK, Weyergang A, Høgset A, Norum OJ, Berstad MB, Vikdal M, Berg K (2010) Photochemical internalization provides time- and space-controlled endolysosomal escape of therapeutic molecules. J Control Release 148(1):2–12 [PubMed: 20600406]
5. Weyergang A, Berstad ME, Bull-Hansen B, Olsen CE, Selbo PK, Berg K (2010) 2015 photochemical activation of drugs for the treatment of therapy-resistant cancers. Photochem Photobiol Sci 14:1465
6. Berg K, Dietze A, Kaalhus O, Høgset A (2005) Site-specific drug delivery by photochemical internalization enhances the antitumor effect of bleomycin. Clin Cancer Res 11(23):8476–8485 [PubMed: 16322311]
7. Norum OJ, Bruland ØS, Gorunova L, Berg K (2009) Photochemical internalization of bleomycin before external-beam radiotherapy improves locoregional control in a human sarcoma model. Int Radiat Oncol Biol Phys 75(3):878–885
8. Hirschberg H, Zhang MJ, Gach HM, Uzal FA, Chighvinadze D, Sun CH, Peng Q, Madsen SJ (2009) Targeted delivery of bleomycin to the brain using photo-chemical internalization of Clostridium perfringens epsilon prototoxin. J Neuro-Oncol 95(3):317–329
9. Mathews MS, Blickenstaff JW, Shih EC, Zamora G, Vo V, Sun CH, Hirschberg H, Madsen SJ (2012) Photochemical internalization of bleomycin for glioma treatment. J Biomed Opt 17(5): 058001 [PubMed: 22612148]
10. Sultan AA, Jerjes W, Berg K, Høgset A, Mosse CA, Hamoudi R, Hamdoon Z, Simeon C, Carnell D, Forster M, Hopper C (2016) Disulfonated tetraphenyl chlorin (TPCS2a)-induced photochemical internalisation of bleomycin in patients with solid malignancies: a phase 1, dose-escalation, first-in-man trial. Lancet Oncol 17(9): 1217–1229 [PubMed: 27475428]
11. Tang Y, McGoron AJ (2009) Combined effects of laser-ICG photothermotherapy and doxorubicin chemotherapy on ovarian cancer cells. J Photochem Photobiol B Biol 97:138–144
12. Zhang W, Guo Z, Huang D et al. (2011) Synergistic effect of chemophotothermal therapy using PEGylated graphene oxide. Biomaterials 32(33):8555–8561 [PubMed: 21839507]
13. Mehtala JG, Torregrosa-Allen S, Elzey BD et al. (2014) Synergistic effects of cisplatin chemotherapy and gold nanorod-mediated hyperthermia on ovarian cancer cells and tumors. Nanomedicine 9(13):1939–1955 [PubMed: 24498890]
14. Madsen SJ, Shih EC, Peng Q, Christie C, Krasieva T, Hirschberg H (2016) Photothermal enhancement of chemotherapy mediated by gold-silica nanoshell-loaded macrophages: in vitro squamous cell carcinoma study. J Biomed Opt 21(1):18004 [PubMed: 26811077]
15. Terentyuk GS, Maslyakova GN, Suleymanova LV, Khlebtsov NG, Khlebtsov BN, Akchurin GG, Maksimova IL, Tuchin VV (2009) Laser-induced tissue hyperthermia mediated by gold nanoparticles: toward cancer phototherapy. J Biomed Opt 14:021016 [PubMed: 19405729]
16. Kennedy LC, Bickford LR, Lewinski NA, Coughlin AJ, Hu Y, Day ES, West JL, Drezek RA (2011) A new era for cancer treatment: gold-nanoparticle-mediated thermal therapies. Small 7(2): 169–183 [PubMed: 21213377]
17. Gobin AM et al. (2007) Near-infrared resonant nanoshells for combined optical imaging and photothermal cancer therapy. Nano Lett 7(7):1929–1934 [PubMed: 17550297]
18. Oldenburg SJ et al. (1998) Nanoengineering of optical resonances. Chem Phys Lett 288:243–247

19. Oldenburg SJ et al. (1999) Infrared extinction properties of gold nanoshells. Appl Phys Lett 75:2897–2899
20. Huang X et al. (2007) Gold nanoparticles: interesting optical properties and recent applications in cancer diagnostics and therapy. Nanomedicine 2:681–693 [PubMed: 17976030]
21. Barua S, Mitragotri S (2014) Challenges associated with penetration of nanoparticles across cell and tissue barriers: a review of current status and future prospects. Nano Today 9:223–243 [PubMed: 25132862]
22. Huynh E, Zheng G (2015) Cancer nanomedicine: addressing the dark side of the enhanced permeability and retention effect. Nanomedicine (Lond) 10(13):1993–1995 [PubMed: 26096565]
23. Fischbach MA, Bluestone JA, Lim WA (2013) Cell-based therapeutics: the next pillar of medicine. Sci Transl Med 5(179):ps7
24. Basel MT, Shrestha TB, Bossmann SH, Troyer DL (2014) Cells as delivery vehicles for cancer therapeutics. Ther Deliv 5(5):555–567 [PubMed: 24998274]
25. Choi MR et al. (2007) A cellular Trojan horse for delivery of therapeutic nanoparticles into tumors. Nano Lett 7(12):3759–3765 [PubMed: 17979310]
26. Owen MR, Byrne HM, Lewis CE (2004) Mathematical modeling of the use of macrophages as vehicles for drug-delivery to hypoxic tumour sites. J Theor Biol 226:377–391 [PubMed: 14759644]
27. Valable S, Barbier EL, Bernaudin M, Roussel S, Segebarth C, Petit E et al. (2008) In vivo MRI tracking of exogenous monocytes/macrophages targeting brain tumors in a rat model of glioma. NeuroImage 40(2):973–983 [PubMed: 18441552]
28. Choi J, Kim HY, Ju EJ et al. (2012) Use of macrophages to deliver therapeutic and imaging contrast agents to tumors. Biomaterials 33(16):4195–4203 [PubMed: 22398206]
29. Baek S-K, Makkouk AR, Krasieva T, Sun C-H, Madsen SJ, Hirschberg H (2011) Photothermal treatment of glioma: an in vitro study of macrophage-mediated delivery of gold nanoshells. J Neuro-Oncol 104:439–448
30. Madsen SJ, Christie C, Hong SJ, Trinidad A, Peng Q, Uzal FA, Hirschberg H (2015) Nanoparticle-loaded macrophage-mediated photothermal therapy: potential for glioma treatment. Lasers Med Sci 30(4):1357–1365 [PubMed: 25794592]
31. Christie C, Madsen SJ, Peng Q, Hirschberg H (2015) Macrophages as nanoparticle delivery vectors for photothermal therapy of brain tumors. Ther Deliv 6(3):371–384 [PubMed: 25853311]
32. Hirschberg H, Madsen SJ (2017) Cell mediated photothermal therapy of brain tumors. J NeuroImmune Pharmacol 12(1):99–106 [PubMed: 27289473]
33. Yang TD, Choi W, Yoon TH, Lee KJ, Lee JS, Han SH, Lee MG, Yim HS, Choi KM, Park MW, Jung KY, Baek SK(2012) Real-time phase-contrast imaging of photothermal treatment of head and neck squamous cell carcinoma: an in vitro study of macrophages as a vector for the delivery of gold nanoshells. J Biomed Opt 17:128003 [PubMed: 23235837]
34. Park H, Yang J, Lee J et al. (2009) Multifunctional nanoparticles for combined doxorubicin and photothermal treatments. ACS Nano 3(10):2919–2926 [PubMed: 19772302]
35. Madsen SJ, Shih EC, Peng Q, Christie C, Krasieva T, Hirschberg H (2016) Photothermal enhancement of chemotherapy mediated by gold-silica nanoshells loaded macrophages; an in vitro squamous cell carcinoma study. J Biomed Opt 21(1):18004 [PubMed: 26811077]
36. Kah JC, Wan RC, Wong KY, Mhaisalkar S, Sheppard CJ, Olivo M (2008) Combinatorial treatment of photothermal therapy using gold nanoshells with conventional photodynamic therapy to improve treatment efficacy: an in vitro study. Lasers Surg Med 40(8):584–589 [PubMed: 18798290]
37. Kuo WS, Chang YT, Cho KC, Chiu KC, Lien CH, Yeh CS, Chen SJ (2012) Gold nanomaterials conjugated with indocyanine green for dual-modality photodynamic and photothermal therapy. Biomaterials 33(11):3270–3278 [PubMed: 22289264]
38. Trinidad AJ, Hong SJ, Peng Q, Madsen SJ, Hirschberg H (2014) Combined concurrent photodynamic and gold nanoshell loaded macrophage-mediated photothermal therapies: an in vitro study on squamous cell head and neck carcinoma. Lasers Surg Med 46(4):310–318 [PubMed: 24648368]

39. Christie C, Molina S, Gonzales J, Berg K, Nair RK, Huynh K, Madsen SJ, Hirschberg H (2016) Synergistic chemotherapy by combined moderate hyperthermia and photochemical internalization. Biomed Opt Express 7(4):1240–1250 [PubMed: 27446650]

40. Kim H, Lee D, Kim J, Kim TI, Kim WJ (2013) Photothermally triggered cytosolic drug delivery via endosome disruption using a functionalized reduced graphene oxide. ACS Nano 7(8):6735–6746 [PubMed: 23829596]

41. Fu J, Wang D, Mei D, Zhang H, Wang Z, He B, Dai W, Zhang H, Wang X, Zhang Q (2015) Macrophage mediated biomimetic delivery system for the treatment of lung metastasis of breast cancer. J Control Release 204:11–19 [PubMed: 25646783]

42. Li S, Feng S, Ding L, Liu Y, Zhu Q, Qian Z, Gu Y (2016) Nanomedicine engulfed by macrophages for targeted tumor therapy. Int J Nanomedicine 11:4107–4124 [PubMed: 27601898]

43. Shin D, Christie C, Ju D, Nair RK, Molina S, Berg K, Krasieva TB, Madsen SJ, Hirschberg H (2017) Photochemical internalization enhanced macrophage delivered chemotherapy. Photodiagnosis Photodyn Ther 21:156–162 [PubMed: 29221858]

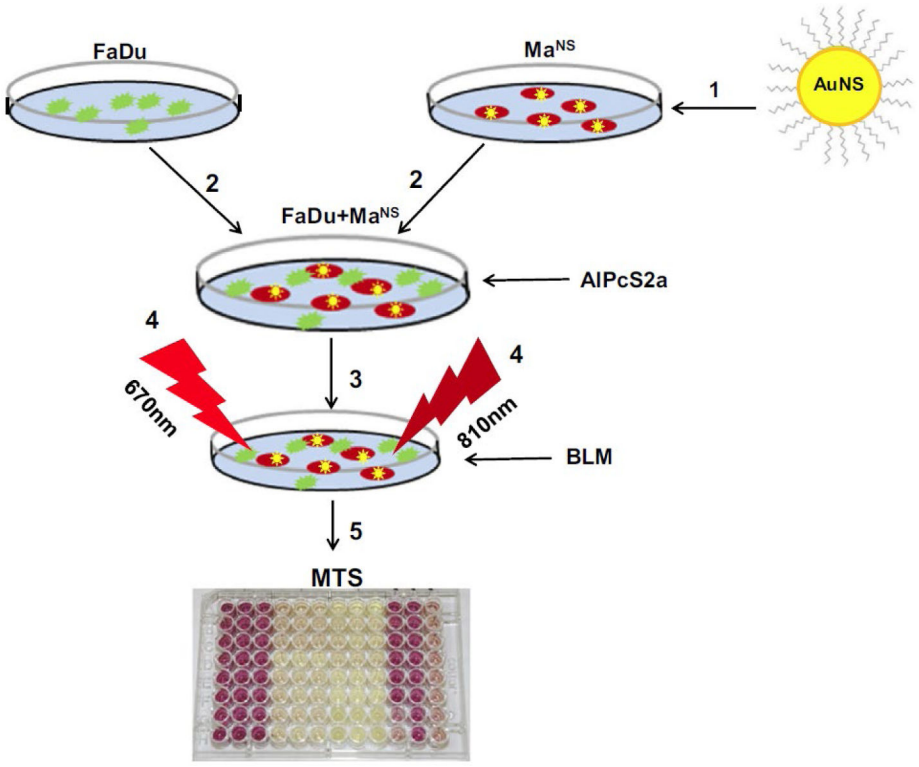

Fig. 1.

Overview of combined PCI-PTT treatment via two wavelength irradiations. (1) PEGylated nanoshells incorporated into Macrophages (Ma) forming nanoshell laden Ma (Ma^{NS}). (2) Ma^{NS} are mixed with FaDu cells to form hybrid monolayers of FaDu-Ma^{NS}. Photosensitizer (AlPcS2a) is added. (3) Bleomycin (BML) at different concentrations is added. (4) Each well is irradiated with either 810 and 670 nm or a combination of the two wavelengths. (5) MTS assay is used to evaluate cell survival

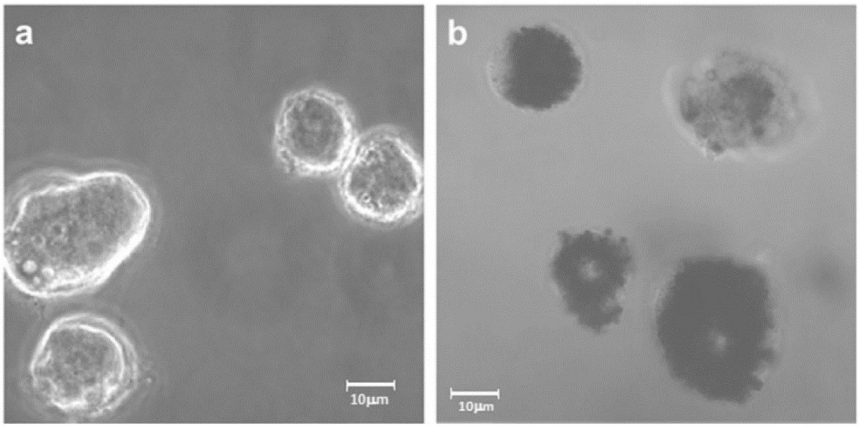

Fig. 2.

Confocal micrographs of internalized PEGylated AuNS nanoshells by Ma. Ma was incubated with 100 μl of PEGylated (2.8 × 1011 particles/ml) nanoshells colloid for 24 h at 37 °C. **a** Empty Ma; **b** Ma with internalized AuNS. Nanoparticles are shown as dark inclusions

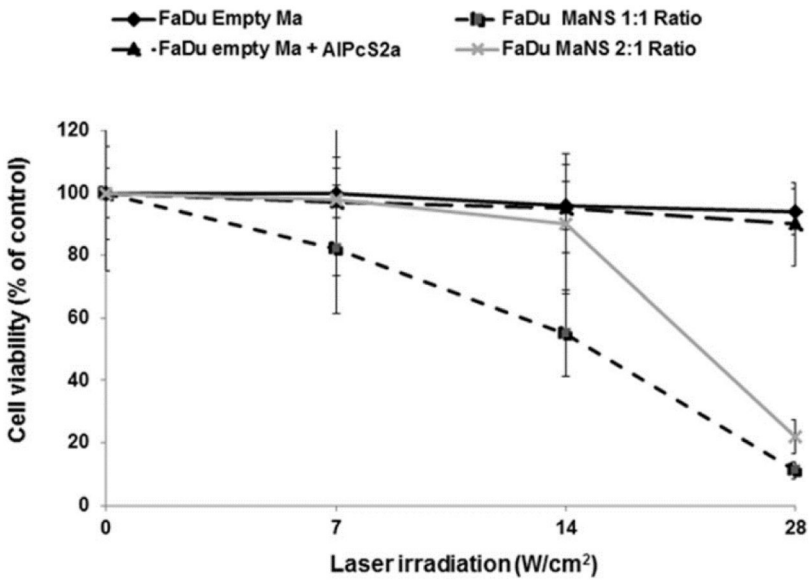

Fig. 3.

Effects of PTT on hybrid monolayers of FaDu-Ma^{NS}. Hybrids were formed with FaDu:Ma^{NS} ratios of either 1:1 or 2:1. NIR laser powers administered at 0, 7, 14, or 28 W/cm^2. Cell viability assessed by MTS assay. Error bars denote standard error

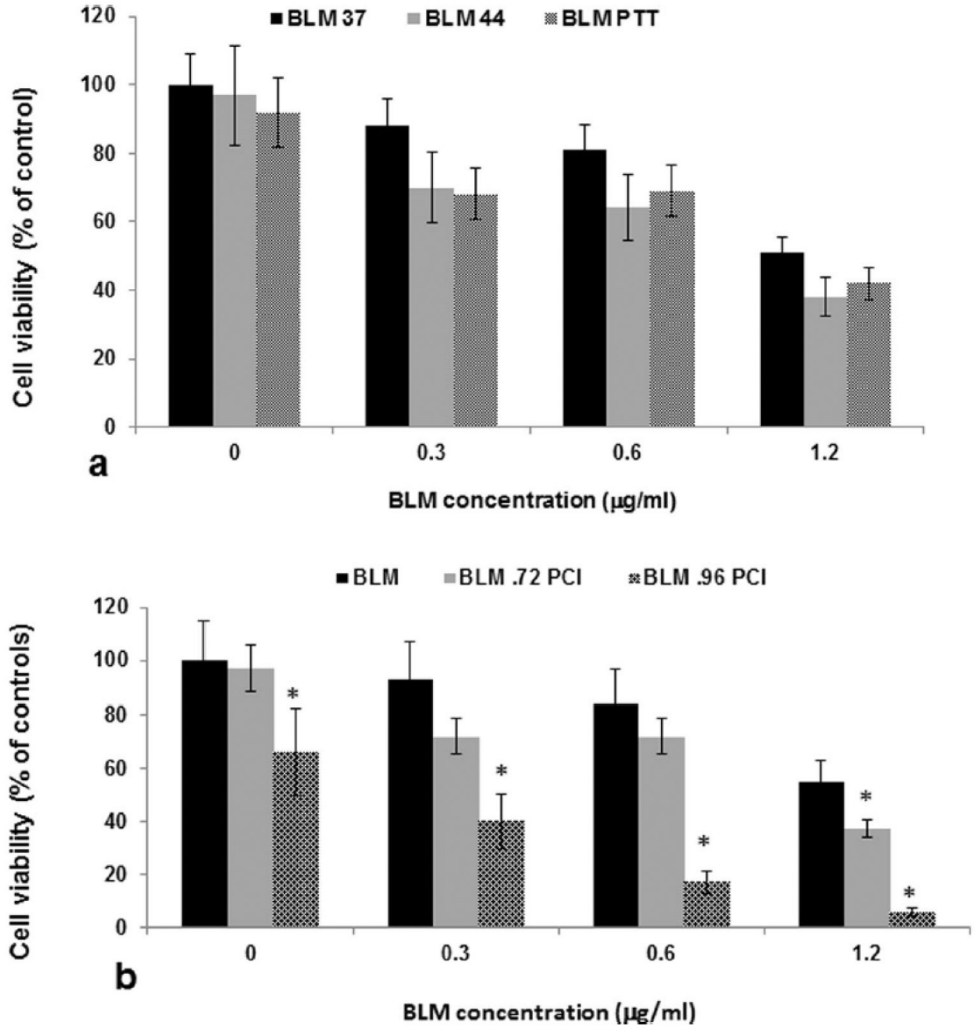

Fig. 4.

Effect of BLM on hybrid monolayers of FaDu-Ma^{NS}. BLM administered at varying concentrations, from 0 to 1.2 μg/ml. FaDu:Ma^{NS} ratio of 2:1 **a** BLM treatment combined with MHT or PTT. External MHT was applied for 45 min at either 37 or 44 °C. PTT was performed with 14 W/cm^2 for 6 min. **b** BLM treatment combined with PCI. Cells were irradiated with λ = 670 nm at exposures of 0, 0.72, or 0.96 J/cm^2. Cell viability was assessed by MTS assay. Error bars denote standard error

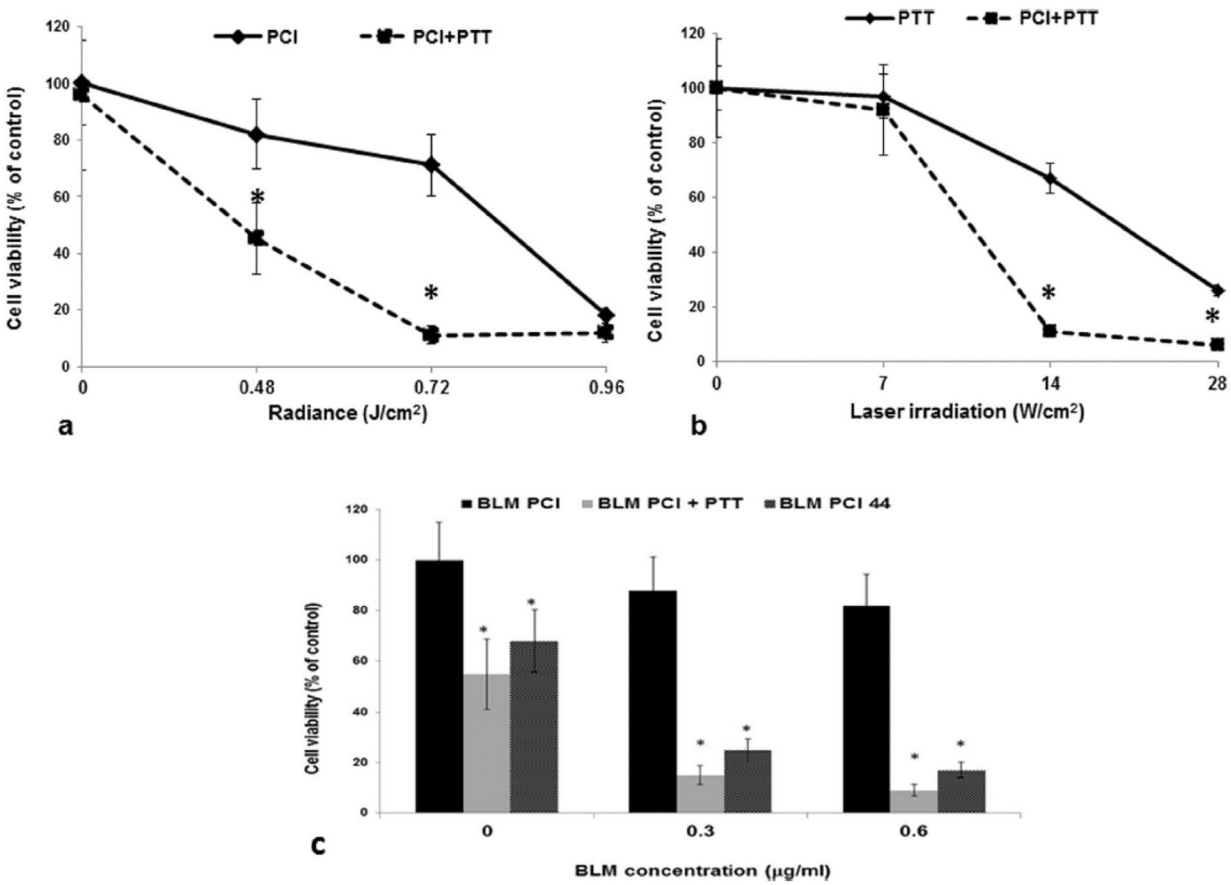

Fig. 5.

Effects of PCI-BLM combined with PTT on hybrid monolayers of FaDu-Ma^{NS}. BLM concentration of 0.6 μg/ml. FaDu:Ma^{NS} ratio of 2:1 **a** PCI, λ = 670 nm laser irradiance of 0–0.96 J/cm^2. PTT NIR laser irradiance of 14W/cm^2. **b** PTT NIR laser irradiance of 0–28 W/cm^2. PCI, λ = 670 nm laser radiance of 0.72 J/cm^2. Cell viability assessed by MTS assay. Error bars denote standard error and *represents significant differences ($p < 0.05$) compared to controls

Table 1

α values for PTT BLM-PCI

BLM concentration	PTT 14 W/cm^2	PTT 28 W/cm^2	MHT 44 °C
0 μg/ml	1.6$^{\#}$ ± 0.14	1.6 ± 0.18	1.44 ± 0.18
0.3 μg/ml	5.0 ± 0.34	1.4 ± 0.14	3.7 ± 0.31
0.6 μg/ml	6.3 ± 0.58	1.5 ± 0.16	4.3 ± 0.39

$^{\#}$ α value.

α value was calculated using the equation ($SF^{PTT} \times SF^{PCI}$)/$SF^{PTT + PCI}$. α values > 1 synergistic effects, values < 1 antagonistic effects, and values = 1 show no or additive effects